ACS APPLIED MATERIALS & INTERFACES

Research Article

www.acsami.org

Sandwich-Type Au-PEI/DNA/PEI-Dexa Nanocomplex for Nucleus-Targeted Gene Delivery in Vitro and in Vivo

Zhenzhen Chen, Lifen Zhang,* Yuling He, and Yanfeng Li*

State Key Laboratory of Applied Organic Chemistry, Key Laboratory of Nonferrous Metals Chemistry and Resources Utilization of Gansu Province, College of Chemistry and Chemical Engineering, Institute of Biochemical Engineering & Environmental Technology, Lanzhou University, Lanzhou 730000, China

Supporting Information

ABSTRACT: Many synthetic Au-based cationic nanoparticles (AuNPs) for nonviral gene delivery show high efficiency in vitro, but their excessive charge density, harsh reducing conditions, and nontarget delivery prevent their application in vivo. Herein, we constructed a sandwich-type layered polyethylenimine (PEI)-coated gold nanocomposite outerlaid with a nucleus-targeted Dexamethasone (Dexa), namely, Au-PEI/DNA/PEI-Dexa nanocomplex, for DNA delivery system using a low molecular weight PEI as a mild reducing agent. The nucleus-targeting Au-PEI/DNA/PEI-Dexa nanocomplex with low positive charge and low cytotoxicity condensed DNA and protected from enzymatic degradation. In vitro transfection studies demonstrated that Au-PEI/DNA/PEI-Dexa nanocomplex exhibited much more efficient nucleus transfection than Au-PEI/DNA/PEI without nucleus-targeted residues and commercially available PEI 25 kDa due to the Dexa targeting of the nucleus. Furthermore, the nanocomplex markedly transfected pTRAIL (TRAIL = tumor-necrosis-factor-related apoptosis-inducing ligand) to tumors in vivo and subsequently inhibited the tumor growth with minimal side effects. These findings suggest that nucleus-targeting Au-PEI/DNA/PEI-Dexa ternary complexes have promising potential in gene delivery.

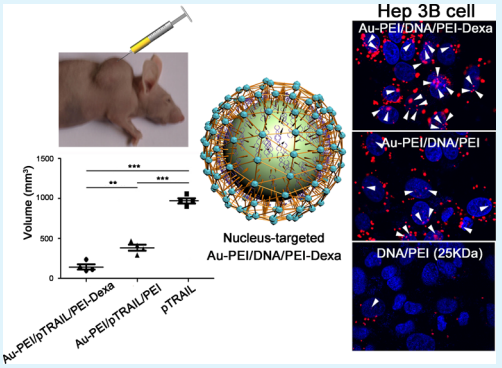

KEYWORDS: *gold nanoparticle, layer-by-layer, nucleus-targeted, polyethylenimine, dexamethasone*

INTRODUCTION

The development of gene therapy over the past three decades has made it one of the most promising technologies to treat human disorders, including both acquired and inherited diseases.[1] The success of gene therapy depends mainly on the gene delivery vectors used. Although these vectors are able to introduce genetic material into specific target cells or tissues, the development of these vectors has been hampered by their lack of efficiency, due to a variety of barriers in extracellular and intracellular spaces.[2−4] These barriers may be overcome by various types of nonviral vectors, including cationic polymers,[5] lipids,[6] peptides,[7] and polyamidoamine (PAMAM)[8] that can form ionic complexes with DNA. Although these nonviral vectors have been found to be safer, less costly, less immunogenic, and easier to produce than viral vectors, their transfection efficiency remains one of the barriers to their application in vivo.[9,10]

The emerging nonviral vectors for gene delivery such as silica,[11] iron oxide,[12] and gold[13,14] nanoparticles are able to settle onto the surface of target cells, facilitating the delivery of DNA.[15] Gold nanoparticles (AuNPs) are of particular interest as vectors for the delivery of both drugs and genes owing to their ease of synthesis, adjustable size, flexible surface modification and bioconjugation, chemical inertness, and low innate cytotoxicity.[16−18] AuNPs can be linked to functional groups, including cationic amino acids,[19] polyethylenimine (PEI),[20] quaternary ammonium chains,[21] 2-aminoethanethiol,[22] and cationic lipids,[23] significantly improving their DNA-binding capacity for in vitro transfection. PEI seems to be particularly effective because it is capable of not only condensing DNA and facilitating cell entry but also enabling endosomal escape by destabilizing the endosomal membrane via osmotic swelling.[24,25] Tewin et al. developed layer-by-layer (LBL) assembled AuNPs by incorporating DNA into complexes with PEI, chitosan, or both, resulting in a 10-fold higher efficiency of DNA transfection than when using polymeric-based gene carriers.[26,27] Unfortunately, all of the above Au-based systems have limitations such as nontargeted delivery or the requirement for harsh reducing reagents during the process of AuNPs synthesis, such as $NaBH_4$. The development of a targeted Au-based delivery system using a mild reducing reagent was therefore of interest to us.

Generally, the nucleus is the main target of polymer-mediated intracellular gene delivery.[28] In nondividing cells, DNA is transported across the nuclear membrane, a barrier to DNA-based gene delivery, via the nuclear pore complex (NPC). The intracellular glucocorticoid receptor regulates the translocation of the receptor−ligand complex into the

Received: June 4, 2014
Accepted: July 14, 2014
Published: July 14, 2014

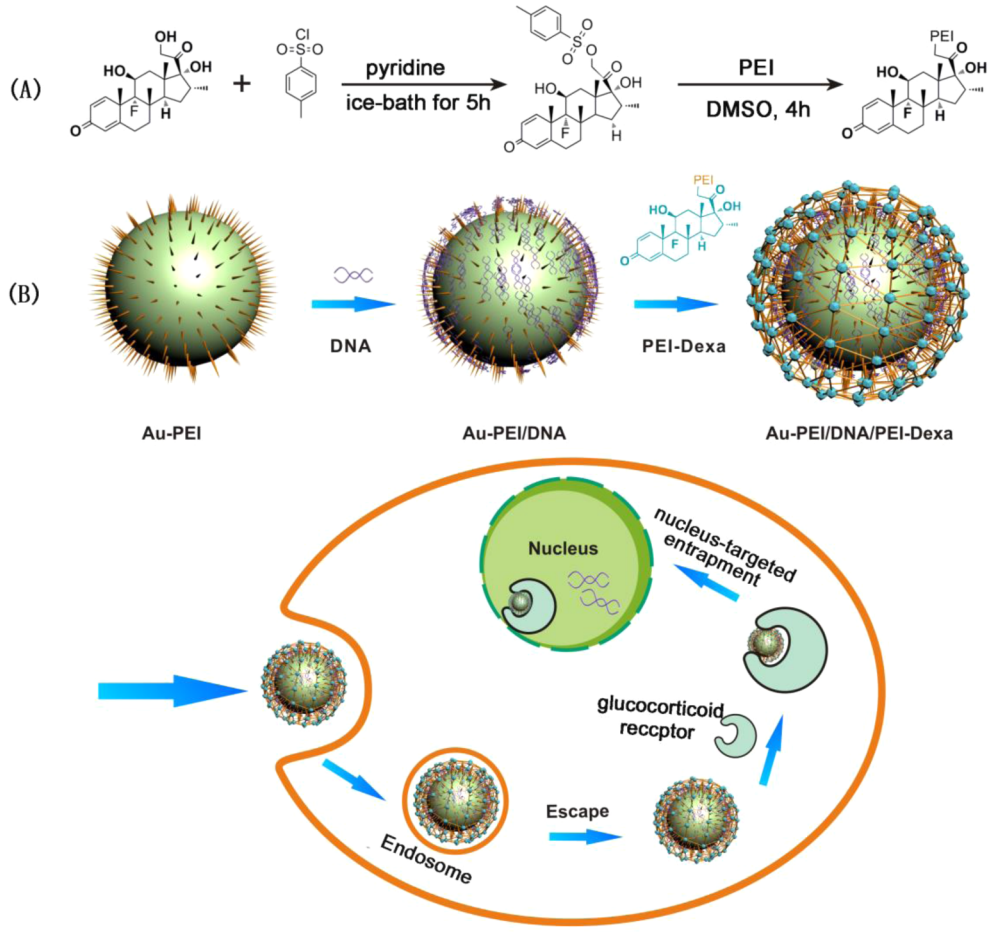

Figure 1. Schematic illustration of PEI-Dexa synthesis (A) and nucleus-targeted sandwich-type Au-PEI/DNA/PEI-Dexa complex for intercellular DNA delivery (B).

nucleus.[29] The NPC was shown to dilate the nuclear pore to 60 nm, facilitating the translocation into the nucleus of the NPC-receptor complex in the presence of the ligand Dexamethasone (Dexa), a potent glucocorticoid steroid.[30] Therefore, Dexa used as nucleus-targeted residues on AuNPs could be useful in enhancing the importing of DNA into the nucleus. The aim of this study was to develop a nucleus-targeting nanosystem based on PEI-functionalized gold nanoparticles (Au-PEI) via LBL assembly method to facilitate nuclear translocation both in vitro and in vivo, which is beneficial in the enhancement of efficient DNA transfection. Herein, a sandwich-type Au-PEI/DNA/PEI-Dexa nanocomposite outerlaid with nucleus-targeting Dexa was proposed and synthesized for efficient nucleus-targeted gene delivery (Figure 1). Positively charged Au-PEI nanoparticles were synthesized from an aqueous solution of linear PEI/$HAuCl_4$ using PEI (1.2 kDa) as a reducing and protective agent without any external reducing agent.[31] Low molecular weight PEI was chosen to overcome the high cytotoxicity of Au-PEI (25 kDa) as well as to possess transfection activities. The physiochemical characterizations of Au-PEI/DNA/PEI-Dexa nanocomplexes were determined in detail. Furthermore, the positive effect of Dexa on the efficient nucleus-targeted in vitro transfection using the nanocomplex into various cell lines was confirmed by flow cytometry and confocal microscopy, Au-PEI/DNA/PEI and PEI 25 kDa used as control. Finally, the in vivo transfection of Au-PEI/pTRAIL/PEI-Dexa carrying pDNA encoding tumor-necrosis-factor-related apoptosis-inducing ligand (TRAIL) in tumor and the inhibition of tumor growth were both evaluated.

EXPERIMENTAL SECTION

Materials. PEI of molecular weight (M_w) 1.2 and 25 kDa, dexamethasone, 4,6-diamidino-2-phenylindole (DAPI), tetrachloroauric (III) acid ($HAuCl_4$), 3-[4,5-dimethylthiazol-2-yl]-2,5-diphenyltetrazolium bromide (MTT), dry pyridine, *p*-toluensulfonyl chloride (PTSA), Flag antibody, and chloroauric acid were purchased from Sigma-Aldrich. Hep3B and 293T cells were kindly provided by Dr. Li (Lanzhou University). Dulbecco's modified Eagle's medium (DMEM), fetal bovine serum (FBS), ethidium bromide, and agarose were obtained from Invitrogen Corporation. DNaseI, DNase reaction buffer, and stop reaction buffer were purchased from Promega. LysoTracker Green DND-26 (Catalog No. L-7526) was purchased from Invitrogen. Transfection reagent was purchased from Mirus Bio LLC. Water used in all experiments was purified using a Milli-Q Plus 185 water purification system (Millipore, Bedford, MA) with a resistivity higher than 18 MΩ cm. pEGFP-C1 (4.7 kb) plasmid driven by the SV40 promoter were from Promega (Madison, WI). pFlag-cmv2 plasmid were purchased from Addgene. All the other chemicals were purchased from Energy Chemical and were used as received.

Synthesis of Au-PEI Nanoparticles. Au nanoparticles were synthesized as described with some modifications.[31] Briefly, 5 mL of PEI (M_w = 1.2 kDa) was added to 5 mL of 1 mM $HAuCl_4$ while stirring at 80 °C in an oil bath. When the reaction mixture became red, it was removed from the oil bath, with stirring continued until the mixture reached ambient temperature. The resulting Au-PEI NPs were purified by dialysis (3500 Da cutoff) against distilled water to remove the unbound PEI.

Synthesis of PEI-Dexa. PTSA (170 mg, 0.9 mmol) in 5 mL of dry pyridine was added dropwise to Dexa (120 mg, 0.3 mmol) in 5 mL of dry pyridine at 0 °C under nitrogen atmosphere, with stirring continued for 5 h at 0 °C. The mixture was added to ice-cold saline and filtered. The precipitate was washed with ice−water and freeze-dried. The resulting Dexa-PTSA product (80 mg, 0.15 mmol) was added to a solution of PEI (M_w = 1.2 kDa) (720 mg, 0.6 mmol) in 5 mL of dimethyl sulfoxide (DMSO) under nitrogen atmosphere and stirred for 4 h at room temperature. The product was dialyzed for 2 d against pure water using a dialysis membrane (MWCO 1000) and freeze-dried. The resulting white product was dissolved in D_2O for ^1H NMR analysis (Bruker AM-400 MHz spectrometer).

Preparation of Au-PEI/DNA/PEI-Dexa. Au-PEI/DNA/PEI-Dexa ternary complexes were prepared by adding 62.5 μL of DNA (0.4 μg/μL) in phosphate-buffered saline (PBS) dropwise to a solution of Au-PEI with various weight ratio of Au-PEI to DNA, followed by incubation at room temperature for 30 min; PEI or PEI-Dexa solution was then added to the above mixture with various w/w ratio, followed by incubation for 30 min at room temperature. The resulting Au-PEI/DNA (weight ratio of (0.2, 0.3, 0.6, 0.9, 1.2)/1), Au-PEI/DNA/PEI (weight ratio of 0.6/1/1(2, 5), and Au-PEI/DNA/PEI-Dexa (weight ratio of 0.6/1/1(2, 5) were prepared. PEI 25 kDa/DNA polyplexes at indicated N/P ratio were used as positive controls in some assays.

Characterization of Au-PEI/DNA/PEI-Dexa. The Z-average hydrodynamic diameter and surface charge of complexes were determined by Zetasizer Nano (Malvern ZS90, UK) at room temperature. The complexes were prepared and combined to yield a volume of 1 mL using DI water. All samples were measured in triplicate. The morphology and size of the Au-PEI, Au-PEI/DNA (w/w ratio, 0.6/1), and Au-PEI/DNA/PEI-Dexa (w/w/w ratio, 0.6/1/2) nanoparticles were analyzed by transmission electron microscopy (TEM) (JEM-2010, JEOL, Japan) at an acceleration voltage of 200 kV. Surface plasmon resonance absorption was determined by UV−vis spectrophotometry (S-3100, Scinco Co., Seoul, Korea) in the range of 400−700 nm. The retardation of DNA by the complexes was assessed by gel electrophoresis, with DNA bands visualized by in vivo imaging (Kodak In-Vivo Imaging System FX Pro). To evaluate the protection of Au-PEI/DNA/PEI-Dexa and Au-PEI/DNA/PEI, 0.5 μg of DNA in Au-PEI/DNA/PEI-Dexa (w/w/w ratio, 0.6/1/1(2, 5)) and Au-PEI/DNA/PEI (w/w/w ratio, 0.6/1/1(2, 5)) were digested with 2 μL of DNase I (5 U/μL) at 37 °C for 30 min. Heparin (50 units/mg of DNA) was added to dissociate the DNA molecules from the complexes, and images were recorded.

Cytotoxicity Assay. Cell viability in the presence of complexes was determined using MTT. Hep3B or 293T cells were seeded in 96-well microassay plates at a density of 5 × 10^3 cells/well in DMEM complete medium. The cells were allowed to grow for 24 h. The original medium was replaced with fresh DMEM complete medium. To each well was added a solution of Au-PEI/DNA/PEI-Dexa, Au-PEI/DNA/PEI, or PEI 25 kDa, with each dosage replicated in quadruplicate. The cells were incubated for 24 h at 37 °C under a humidified atmosphere of 95% air and 5% CO_2. MTT reagent (20 μL in PBS, 5 mg/mL) was added to each well, and the cells were incubated for another 4 h at 37 °C. To each well was added 100 μL of DMSO to dissolve the crystals, and the absorbance of the solution in each well at 570 nm was recorded using a Microplate Reader (Bio-Rad model 550). Here, the absorbance of the Au-based complex self has been already deducted.

In Vitro Transfection. Hep3B or 293T cells were seeded in 12-well plates at a density of 4 × 10^4 cells/well and cultured for 24 h. The culture medium was replaced with fresh medium, and the cells were transfected with gene delivery complexes containing 1 μg of pEGFP for 4 h. The transfection medium was replaced with normal culture medium, and the cells were cultured for an additional 48 h. The medium was removed, and the cells were washed with complete medium and trypsinized, and pEGFP expression was quantified by confocal laser scanning microscopy (Olympus FV1000) and flow cytometry (BD FACSCalibur). Nuclei were stained with blue molecular Hoechst stain.

Conjugation of Cy5 to DNA. We conjugated DNA with Cy5 using Label IT Nucleic Acid Labeling Kits, which were purchased from Mirus Bio Corporation. Briefly, molecular biology-grade H_2O, 10X Labeling Buffer A, pFlag-cmv2 plasmid, and Label IT Reagent were mixed together and incubated at 37 °C for 1 h. Then the total volume was increased to 200 μL with 1X Mirus Labeling Buffer A. And then 0.1 L of 5 M NaCl and 2 L of ice-cold 100% ethanol was added to the Labeling reaction. After 30 min of incubation at −20 °C, we centrifuged to pellet the Labeled DNA, washed once with 70% ethanol, air-dried extensively, and finally resolved with molecular biology-grade H_2O.

Cellular Uptake. The intracellular uptake of Au-PEI/DNA/PEI-Dexa (w/w/w, 0.6/1/2) was assessed by flow cytometry, using PEI/DNA (N/P, 10/1) and Au-PEI/DNA/PEI (w/w, 0.6/1/2) as positive controls. These complexes were incubated with Cy5-labled pDNA (1 μg/well) at room temperature for 30 min. Hep3B cells were seeded at a density of 1 × 10^5 cells/well in six-well plates and cultivated overnight at 37 °C with 5% CO_2. The medium was exchanged, and the polyplex solutions in fresh medium were added to the cells and incubated for 4 h. The cells were washed three times with PBS, trypsinized, and harvested by centrifugation at 1000 rpm for 3 min. Finally, the harvested cells were resuspended in PBS buffer and analyzed by flow cytometry. The cells were gated (G1) on forward scatter/side scatter (FSC-H/SSC-H) dot plots, and the fluorescence of each cell sample was measured in the Cy5 channel. For each sample, 1 × 10^4 cells were counted, and the experiment was repeated three times. Differences in cellular uptake were calculated, with p values less than 0.05 considered statistically significant.

Intracellular Trafficking and Localization. Layer-by-layer assemblies of Cy5-labled pDNA with PEI, Au-PEI, or PEI-Dexa were synthesized to form PEI/DNA, Au-PEI/DNA/PEI, and Au-PEI/DNA/PEI-Dexa complexes, respectively. To colocalize the complexes Hep3B cells were seeded at a density of 3 × 10^4 cell in 24-well plates and cultured for 24 h. The cells were treated with PEI/DNA (N/P, 10/1), Au-PEI/DNA/PEI (w/w/w, 0.6/1/2), or Au-PEI/DNA/PEI-Dexa (w/w/w, 0.6/1/2), followed by incubation with LysoTracker Green for 20 min to label lysosomes and DAPI for 15 min to label the cell nuclei.

Nucleocytoplasmic. Hep3B cells were collected and washed by PBS and incubated in 250 μL of lysis buffer (10 mM HEPES-NaOH, 10 mM KCl, 1.5 mM $MgCl_2$, 0.5 mM β-mercaptoethanol, pH 7.9) for 15 min. 10% NP-40 (5 μL) was added for 2 min of incubation, and the samples were separated by centrifuge at 16 000 g for 15 min. The pallet was resuspended with nuclei extract buffer (10 mM Tris-HCl, 420 mM NaCl, 0.5% Nonidet P-40, 1 mM PMSF, 1 mM DTT, 2 mM $MgCl_2$, protease inhibitors, pH 7.6) for 20 min incubation. Finally, 15 min of centrifuging was performed, and the pallet was nuclear section.

TRAIL Cloning. Human mRNA was extracted from monocyte cell line THP1 using Trizol reagent according to standard procedure (http://tools.lifetechnologies.com/content/sfs/manuals/trizol_reagent.pdf). cDNA was obtained by reverse transcription polymerase chain reaction (PCR) from mRNA and served as template for TRAIL cloning. Primers were designed and purchased from Sangon Company (Shanghai, China). PCR product was separated by agarose electrophoresis and purified for TRAIL segment, which was then digested and inserted into Flag-cmv2 vector. After confirming by DNA sequencing, Flag-TRAIL was assembled into nanoparticle.

In Vivo Transfection. Female Balb/c nude mice were maintained in a sterile environment. Three groups of tumor-bearing mice (four per group) were used: group 1, Au-PEI/pTRAIL/PEI-Dexa; group 2, Au-PEI/pTRAIL/PEI (TRAIL with PEI); and group 3, pTRAIL. The mice were subcutaneously injected with 1 × 10^6 Hep3B tumor cells. Tumor size was measured every 5 d, with tumor volumes (V) determined by measuring the length (l) and width (w) ($V = \pi/6lw^2$). When the tumor volumes reached 150−200 mm^3, the complexes were directly injected into the tumors. Differences in tumor volume were calculated by one-way ANOVA, with p values less than 0.05 considered statistically significant. All animal experiments complied with the requirements of the National Act on the Use of Experimental Animals (People's Republic of China). The animals were killed 2 d

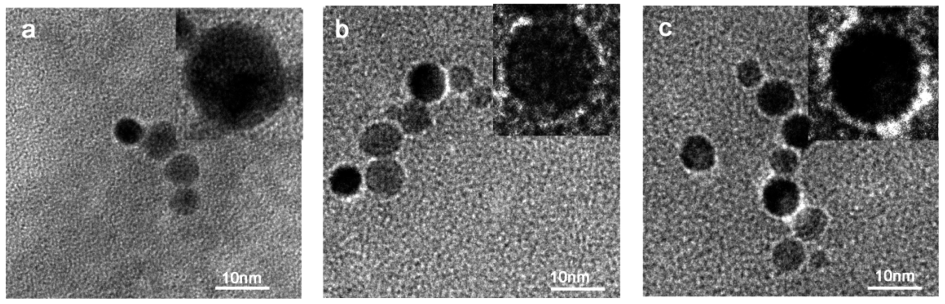

Figure 2. Transmission electron microscopic images of (a) Au-PEI, (b) Au-PEI/DNA, and (c) Au-PEI/DNA/PEI-Dexa. (insets) Higher magnification micrographs of the assembled nanoparticles.

Table 1. Size and Zeta Potential of the Complexes at Various Weight Ratios

complexes	weight ratio	size[a] (nm ± S.D.)	zeta potential[a] (mV ± S.D.)
PEI 25 kDa/DNA	10/1	179 ± 8.21	17 ± 2
Au-PEI		5.7	18.3 ± 1.5
Au-PEI/DNA	0.2/1	10.4 ± 1.01	−17 ± 3.2
Au-PEI/DNA	0.3/1	19 ± 2.75	−12 ± 2.7
Au-PEI/DNA	0.6/1	110.9 ± 7.62	6 ± 0.2
Au-PEI/DNA	0.9/1	59.1 ± 3.72	15 ± 2.8
Au-PEI/DNA	1.2/1	65.2 ± 6.33	17 ± 1.7
Au-PEI/DNA/PEI-Dexa	0.6/1/1	99.2 ± 7.33	8 ± 0.8
Au-PEI/DNA/PEI-Dexa	0.6/1/2	56.2 ± 6.91	12 ± 0.1
Au-PEI/DNA/PEI-Dexa	0.6/1/5	38.2 ± 1.56	15 ± 1.3
Au-PEI/DNA/PEI	0.6/1/1	87.3 ± 6.16	9.25 ± 1.1
Au-PEI/DNA/PEI	0.6/1/2	55.3 ± 5.37	11.3 ± 0.6
Au-PEI/DNA/PEI	0.6/1/5	40.8 ± 2.47	14.3 ± 0.7

[a]Note: The results of zeta potential and size represent mean ± standard deviation (n = 3).

after the last treatment. The tumors were excised and formalin-fixed for next immunohistochemistry or homogenized in lysis buffer for Western blotting assays.

Immunohistochemistry. The 5 μm thick sections were obtained using formalin-fixed tumor tissue. The sections were deparaffinized in xylene and rehydrated in graded alcohols and distilled water. After treatment with 3% hydrogen peroxide for 10 min, the slides were processed for antigen retrieval by a standard microwave heating technique and then blocked with 10% donkey serum for 30 min. The sections were incubated overnight at 4 °C with a 1:500 dilution of Flag antibody (Sigma). The sections were washed and incubated with secondary antibody and the standard 3,3′-diaminobenzidine (DAB) substrate. All sections were counterstained with hematoxylin.

Western Blotting. Tumor cell lysates were subjected to sodium dodecyl sulfate polyacrylamide gel electrophoresis. After electrophoretic separation, the proteins were transferred to nitrocellulose membranes, which were blocked with 8% skim milk for 1 h and incubated with primary anti-Flag antibody overnight at 4 °C. After three washes with TBST (130 mM NaCl, 20 mM Tris, 0.1% Tween, pH 7.6) for 5 min each, the nitrocellulose membranes were incubated with horseradish peroxidase (HRP)-conjugated secondary antibody at room temperature for 1 h, and then visualized by incubation with HRP substrates.

TRAIL Real-Time PCR. After treated with Au-PEI/pTRAIL/PEI, Au-PEI/pTRAIL/PEI-Dexa, or with pTRAIL only, tumor cells injected mice were sacrificed, and many organs were isolated. Organs were homogenized with Trizol reagent (Life Technology) and segregated by adding chloroform. Then the aqueous phage was obtained, and isopropanol and 75% ethanol were added sequentially. Finally the RNA pallet was dissolved by RNase-free double-distilled water (ddH_2O). Then cDNA was obtained with mRNA served as template by reverse-transcription according to standard process provided by promega, and TRAIL expression was determined with real-time quantitative PCR with ABI 7300. TRAIL real-time PCR primer was designed and purchased from Sangon Company (Shanghai, China).

RESULTS AND DISCUSSION

Preparation of Au-PEI/DNA/PEI-Dexa. The procedure used to prepare Au-PEI/DNA/PEI-Dexa complexes is illustrated in Figure 1. PEI was selected as the polycation to

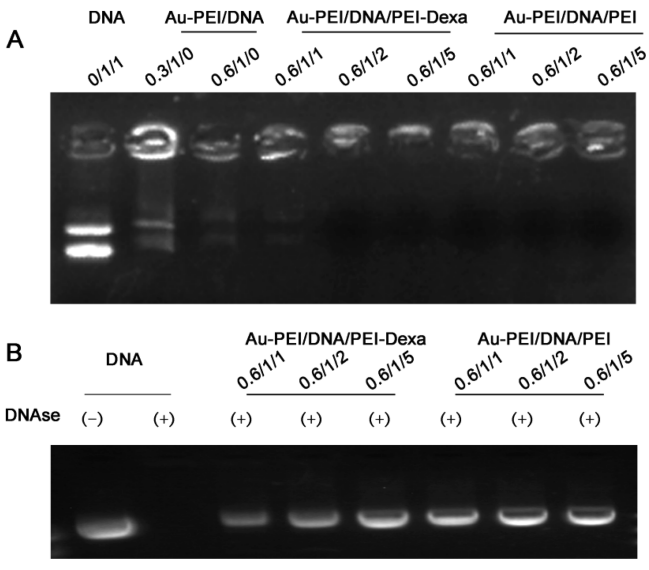

Figure 3. Characterizations of the Au-based complexes. Gel electrophoresis for capability of binding DNA (A) and DNase I digestion (B) results.

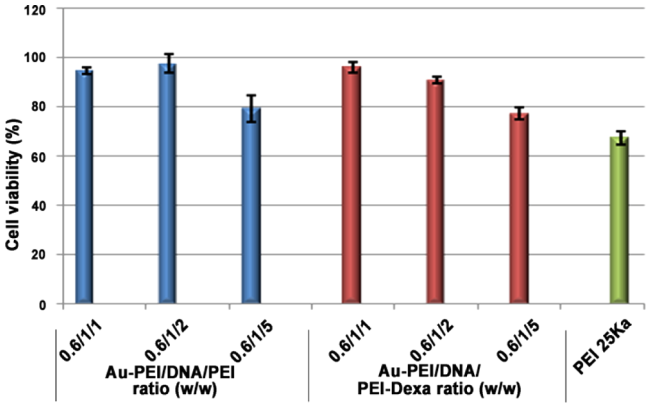

Figure 4. Cell viability determined by MTT assay. Cells were treated with the complex at the weight ratios as indicated, a dose of 1 μg/well of pEGFP was used. Percentage of viability of cells was expressed relative to free cell. The results represent mean ± standard deviation (n = 4).

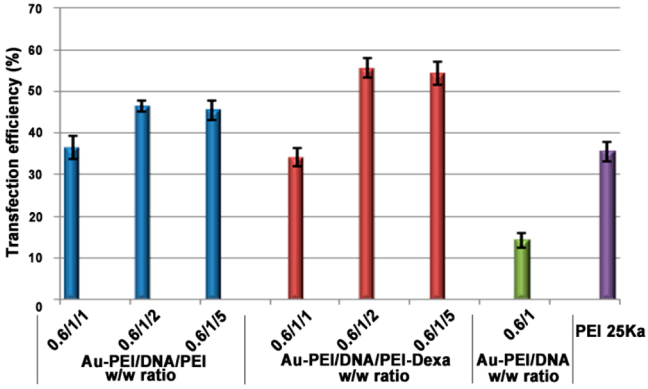

Figure 5. Gene delivery efficiency in vitro. Transfection efficiency of complexes on Hep3B cells at indicated weight ratio, used PEI 25 kDa as positive control. Transfection was performed at a dose of 1 μg/well of pEGFP. The results represent mean ± standard deviation (n = 3).

cap DNA in the complex, because PEI can form stable complexes with nucleic acids by electrostatic interactions and has a strong endosomal escape capacity due to the so-called proton sponge effect.[32] Au-PEI and PEI-Dexa were designed and prepared, followed by LBL assembly with DNA. The synthesis of Au-PEI vehicles was previously reported to be hampered by the intricate process and the requirement for harsh reducing reagents such as $NaBH_4$.[910] In contrast, we synthesized Au-PEI by a convenient, recently developed one-step method. Low molecular weight PEI (1.2 kDa) was both the reducing agent and stabilizer in the generation of PEI-capped AuNPs (Au-PEI) and would form a stable complex with DNA by electrostatic interactions with low cytotoxicity. PEI-Dexa was successfully prepared via a one-step reaction of Dexa-PTSA and PEI at room temperature and was confirmed by ^{1}H NMR spectrum (Supporting Information, Figure S1).

The assembled nanocomplex of Au-PEI/DNA/PEI-Dexa was negatively stained with uranyl acetate and characterized by TEM so that the polymer shells appeared white against the stained background, Au-PEI and Au-PEI/DNA complex used as control. TEM results demonstrated that most nanoparticles remained dispersed (Figure 2). The formation of spherical particles of Au-PEI, ~6 nm in size, was observed in Figure 2a, suggesting the stabilization of PEI on AuNPs. After successful assembly of DNA and subsequent addition of PEI, high-magnification TEM images of DNA-coated AuNP-PEI and DNA/PEI-Dexa (or PEI) coated AuNP-PEI showed that the nanoparticles had a cocoonlike structure, indicating that the sandwich-type nanocomplex was successfully structured based on AuNPs.

Characterization of Au-PEI/DNA/PEI-Dexa Ternary Complexes. The LBL-assembled ternary Au-PEI/DNA/PEI-Dexa complexes were characterized by dynamic light scattering (DLS), gel electrophoresis, and UV−vis spectra. As a starting point, Au-PEI/DNA complexes with various Au-PEI/DNA weight ratios ranging from 0.2/1 to 1.2/1 were designed and tested to generate complexes with weakly positive surface charges that could be used as a platform for the addition of positively charged PEI-Dexa.

The formation of Au-PEI/DNA complexes was confirmed by surface charge analysis and DLS. The surface charges of Au-PEI and Au-PEI/DNA (w/w, 0.2/1) complexes were measured as +18.3 ± 1.5 and −17 ± 3.2 mV, respectively (Table 1). As the weight ratio of Au-PEI/DNA increased, the surface charge of Au-PEI/DNA complexes, which was initially negative, gradually became positive. Au-PEI/DNA (w/w, 0.6/1) complexes with a weakly positive surface charge of 6 mV and probably looser structure, as shown by a large hydrodynamic size of about 110 nm, were selected here for further being assembled with PEI or PEI-Dexa through ionic interactions with partial negatively charged DNA. With increasing addition of PEI or PEI-Dexa coating, the diameter of the AuNPs slightly decreased due to the efficient condensation with Au-PEI/DNA.

The UV−vis spectra of Au-PEI, Au-PEI/DNA, and Au-PEI/DNA/PEI-Dexa complexes showed increased surface plasmon resonance (SPR) bands at 524, 527, and 541 nm, respectively (Supporting Information, Figure S2). Resonance curves have been shown to shift to higher wavelengths as AuNPs became aggregated or the thickness of the adsorbed molecules increased.[33,34] The slight red shift in the SPR band after coating with DNA and PEI-Dexa indicated that the complexes were assembled LBL, without further aggregation of the Au-PEI and Au-PEI/DNA clusters, and that most nanoparticles remained dispersed, in agreement with the DLS and TEM results. All of these results indicated the successful formation of a stable Au-PEI/DNA/PEI-Dexa complex.

The successful electronic interaction between negatively charged DNA and positively charged Au-PEI and PEI-Dexa coating was further evaluated by gel electrophoresis. The efficiency of loading nucleic acid was strongly dependent on its interaction with cationic polymers. Figure 3A shows that compared to naked DNA, although Au-PEI/DNA at a w/w ratio of 0.3/1 and 0.6/1 significantly reduced DNA mobility, some noncomplexed DNA molecules were visible. With addition of PEI-Dexa or PEI, DNA was more tightly and completely complexed, suggesting that the residual negative charges of DNA molecules of Au-PEI/DNA complexes were completely neutralized by the addition of cationic polymers. It is interesting that the shielded PEI-Dexa or PEI on Au-PEI/DNA complex not only condensed DNA completely but also protected DNA from DNase I enzymatic degradation (Figure 3B). These results mean that the sandwich-type complexes were more efficient at protecting the nucleic acid payloads from uptake by the reticuloendothelial system (RES) and passive tumor-targeting by enhanced permeation and retention (EPR).[35]

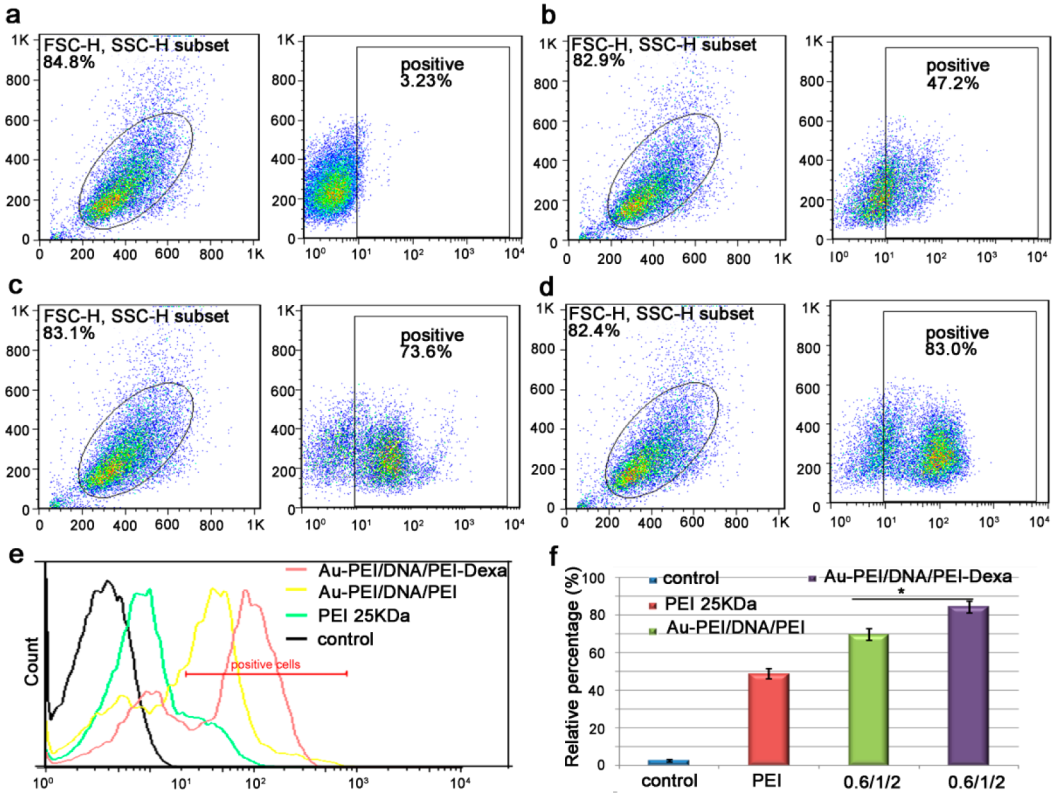

Figure 6. Flow cytometry measurement of the intracellular uptake of vector/Cy5-labled pDNA polyplexes in Hep3B cells. (a) Control cells without treatment (naked DNA). (b) PEI(25 kDa)/DNA (N/P, 10/1). (c) Au-PEI/DNA/PEI (w/w/w, 0.6/1/2). (d) Au-PEI/DNA/PEI-Dexa (w/w/w, 0.6/1/2). (e) Histogram subtraction of cells with Cy5 fluorescence. (f) Relative percentage of the Cy5-labled pDNA of within the selected gate. Transfection was performed at a dose of 1 μg of Cy5-labled pDNA. Data are presented as mean values ± SD (n = 3, *: $p < 0.05$).

Cytotoxicity. The biocompatibility of a delivery vector is critical for its potential clinical application in gene therapy. The cytotoxicity of Au-PEI/DNA/PEI-Dexa complexes toward Hep3B cells was evaluated using MTT. Cells were treated with Au-PEI/DNA/PEI or Au-PEI/DNA/PEI-Dexa under identical conditions to initiate the transfection process. MTT assays showed that the viability of cells transfected was approximately above 80% (Figure 4). The biocompatibility of Au-PEI/DNA/PEI or Au-PEI/DNA/PEI-Dexa may be related to its method of synthesis, which used low molecular weight PEI, a mildly reductive and stable reagent. Conjugating PEI to AuNPs would increase its effective molecular weight.[20] Moreover, the reduced number of primary amines of PEI for AuNPs may be responsible for the stabilization and low cytotoxicity of the entrapped AuNPs. The very similar cell viability was observed for the 293T cells (Supporting Information, Figure S3).

In Vitro Transfection. The transfection efficiency of Au-PEI/DNA/PEI-Dexa complexes into Hep3B and 293T cells in the presence of serum was evaluated by assessing GFP expression by the pEGFP plasmid via confocal laser scanning microscopy (CLSM) and flow cytometry analysis. Au-PEI/DNA/PEI and branched PEI 25 kDa/DNA were used as positive controls. In complete medium, Au-PEI/DNA/PEI-Dexa at a weight ratio of 0.6/1/2 showed the highest reporter gene expression (57%) in Hep3B cells, which was 10% higher than the efficiency of Au-PEI/DNA/PEI (0.6/1/2), about 300% times the expression levels of Au-PEI/DNA (0.6/1) and 50% times the expression of PEI 25 kDa (Figure 5). The significantly PEI-Dexa-induced enhancement of efficiency was due to its Dexa nucleus-targeted enhanced translocation into the nucleus. Similar results were observed in 293T cells (Supporting Information, Figure S4).

To gain further insight into the effect of DNA content on transfection efficiency, we transfected complexes containing 0.6 mg of Au-PEI and 2 mg of PEI-Dexa, as well as different amounts of DNA, in the presence of serum (Supporting Information, Figure S5a–d). The strongest fluorescence intensity of pEGFP expression was observed when the cells were treated with Au-PEI/DNA/PEI-Dexa (w/w/w, 0.6/1/2). Further increase of DNA content gradually reduced the efficiency of the ternary complex, which was also confirmed by flow cytometry analysis (Supporting Information, Figure S5e) and is consistent with the previous report.[2] Taken together, these results indicate that Au-PEI/DNA/PEI-Dexa (0.6/1/2) exhibited the highest relative efficiency as well as low cytotoxicity.

Cellular Uptake. Generally, better cellular uptake of carrier–cargo polyplex should enhance gene delivery and expression. We therefore assessed the cellular uptake behavior of Au-PEI/DNA/PEI-Dexa by flow cytometry using Cy5-labled pDNA, Au-PEI/DNA/PEI without nuclei target residue and PEI 25 kDa/DNA used as control. As shown in Figure 6, 72.9% of the Hep3B cells transfected with Au-PEI/DNA/PEI (w/w of 0.6/1/2) as a vector displayed a Cy5-derived red fluorescence signal, significantly higher than that of PEI 25 kDa (46.8%), indicating that the former had higher cellular uptake ability. The cellular uptake of Au-PEI/DNA/PEI was significantly enhanced in the presence of Dexa residues with the highest cellular uptake (82.5%) observed for Au-PEI/DNA/PEI-Dexa

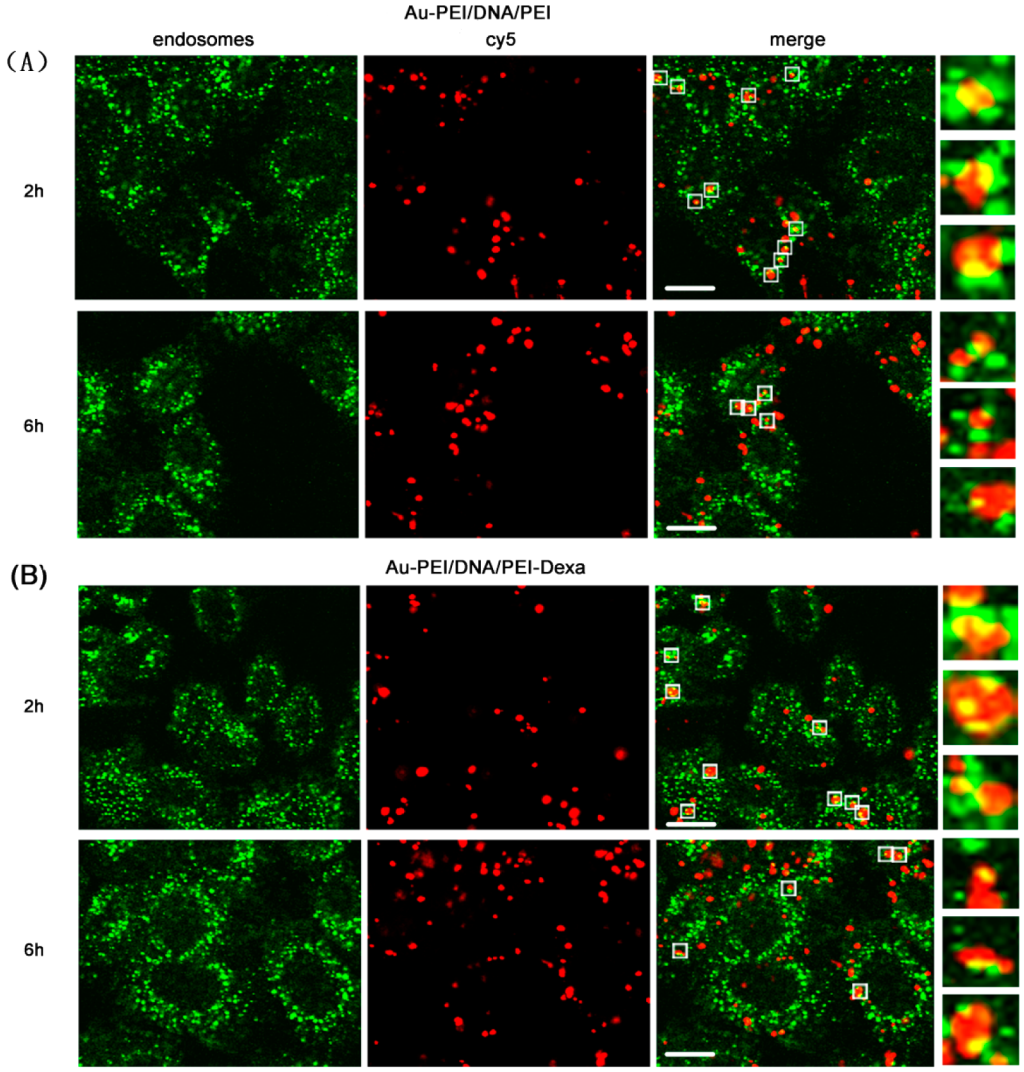

Figure 7. Internalization and subcellular localization of the Cy5-labled pDNA (1 μg/well) with Au-PEI/DNA/PEI (w/w/w, 0.6/1/2) (A) and Au-PEI/DNA/PEI-Dexa (w/w/w, 0.6/1/2) (B) complex in Hep3B cells recorded after 2 or 6 h of gene transfection (green: LysoTracker Green used to label late endosomes and lysosomes; red: Cy5-labled pDNA; yellow: colocalization). Bars =15 μm.

(w/w/w, 0.6/1/2). Thus, the cellular uptake of the ternary complexes corroborated the results of gene transfection.

Internalization and Subcellular Localization. Once the Au-PEI/DNA/PEI-Dexa complex reaches the interior of the cells, it is necessary to understand the efficient cellular internalization of complexes involving nonviral vehicles. To dynamically track the localization of Au-PEI/DNA/PEI and Au-PEI/DNA/PEI-Dexa complexes inside the cell, DNA was labeled with the red fluorescent probe Cy5, while late endosomes and lysosomes were stained with LysoTracker Green. The location of the Au-based DNA complexes and DNA could be clearly seen by colocalization.

As shown in Figure 7, the Au-PEI/DNA/PEI and Au-PEI/DNA/PEI-Dexa complexes were mainly located in the endosomes at 2 h post-transfection, indicating that the complexes were trapped in the endosome after internalization via endocytosis. After 6 h of incubation, few Cy5 signals remained in the endosomes, with most dispersed in the cytoplasm. These changes suggested that the escape of complexes from endosomes may be due to the "proton sponge effect" of PEI and is not related to PEI-Dexa.[36] This finding is in agreement with previous studies, showing that PEI-functionalized Au nanoparticles could release DNA from endosomes.[2]

Intracellular Trafficking. Intracellular trafficking is crucial for gene delivery. Assembly with PEI-Dexa markedly enhanced the transfection efficiency and cellular uptake of Au-PEI/DNA, suggesting that the Dexa residues may act as nuclear localization signals and facilitate the translocation of pDNA into the nucleus, increasing transgenic expression. To confirm this hypothesis, the intracellular location and delivery processes of Au-based DNA complexes were evaluated by dynamic localization of the attached DNA. To monitor Au-based complexes in cells, DNA was labeled with the red fluorescent probe Cy5 using the nick translation method, whereas nuclei were stained with DAPI. By monitoring the location of Au-based DNA complexes, it was determined that these complexes colocalized with other organelles. PEI was used as positive control. Using the Au-PEI/DNA/PEI-Dexa complexes, we found that DNA was transported into the nucleus even 2 h post-transfection, with greater colocalization observed at longer time points (Figure 8A), indicating increased levels of translocation into the nucleus. Au-PEI/DNA and Au-PEI/DNA/PEI complexes showed a similar trend. In contrast, when

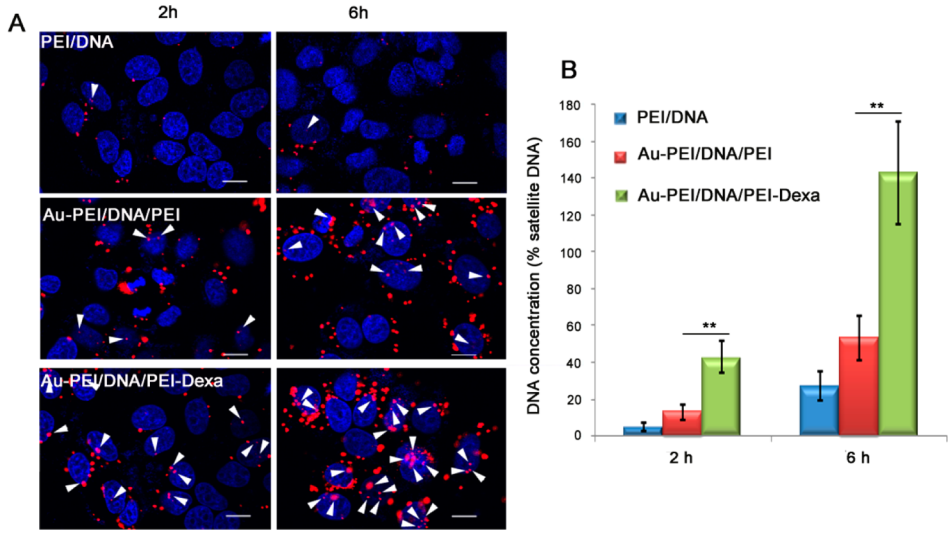

Figure 8. (A) Intracellular localization of PEI/DNA, Au-PEI/DNA/PEI (w/w/w, 0.6/1/2), and Au-PEI/DNA/PEI-Dexa (w/w/w, 0.6/1/2) in Hep3B cells after gene transfection for 2 or 6 h (red: Cy5-labled pDNA; blue: DAPI stained cell nuclei; pink: colocalization). A dose of 1 μg/well of Cy5-labled pDNA was used. White arrows show colocalization of nucleus and plasmid. Bars =15 μm. (B) Intranuclear concentration of pFlag-cmv2 in Hep3B cells treated by PEI/DNA, Au-PEI/DNA/PEI (w/w/w, 0.6/1/2), and Au-PEI/DNA/PEI-Dexa (w/w/w, 0.6/1/2) for 2 or 6 h. Nuclear sections were purified by nucleocytoplasmic separation and examined Flag-cmv2 relative concentration to human satellite DNA, a good control for cellular DNA detection.

we transfected PEI/DNA complexes, we found that only a small amount of DNA colocalized with the nucleus at 2 h post-transfection, with no obvious increases even at 6 h. This ability of Au-based nanoparticles to enhance translocation is consistent with previous findings.[20] Following LBL assembly of PEI-Dexa instead of PEI, we observed that the number of fluorescence dots dramatically increased in and around the nucleus. The higher translocation activity of Au-PEI/DNA/PEI-Dexa was likely due to the positive impact of Dexa on nuclear localization. In summary, efficient translocation of the Au-PEI/DNA/PEI-Dexa complex into the nucleus may have resulted in effective transfection.

To further analyze the nucleus-targeted property of this new system, we performed nucleocytoplasmic separation and examined the concentration of pFlag-cmv2 in nuclear section (Figure 8B). We transfected Hep3B cells by PEI/DNA, Au-PEI/DNA/PEI, and Au-PEI/DNA/PEI-Dexa for 2 and 6 h, collected the cells, and then extracted the nuclear section. The concentration of pFlag-cmv2 in nucleus was examined by real-time PCR using nuclear section as template, and sequence specific primers were designed according to pFlag-cmv2 sequence. The results demonstrated that Au-PEI/DNA/PEI-Dexa exhibited highest copy number of pFlag-cmv2 and delivery efficiency, indicating the enhanced nucleus-targeted property of Dexa, which is in agreement with the confocal data.

Effectiveness of Gene Delivery in Vivo. Because of its excellent transfection ability and low toxicity in vitro, we further tested whether Au-PEI/DNA/PEI-Dexa (w/w/w, 0.6/1/2) carrying therapeutic DNA could inhibit tumor growth in vivo. TRAIL is a member of the horseradish peroxidase (HRP) ligand superfamily[37] that may act as a potent anticancer agent. Transfection of this gene has been shown to selectively induce the apoptosis of tumor cells but not of healthy, nontransformed cells.[38,39] Moreover, TRAIL was shown to induce apoptosis in adjacent tumor cells owing to a bystander effect.[40] To assess this property in our system, TRAIL was cloned into Flag-cmv2 vector to obtain pFlag-cmv-TRAIL (pTRAIL), and pTRAIL was assembled into Au-PEI-based nanoparticle. The Au-PEI/pTRAIL/PEI-Dexa complex was injected into mice bearing Hep3B tumor cells, using Au-PEI/pTRAIL/PEI and pTRAIL as positive controls. Crystal violet assays showed that Au-PEI/pTRAIL/PEI-Dexa (w/w/w, 0.6/1/2) was cytotoxic to Hep3B cells in vitro: 5 d after gene transfection, the proliferation of Hep3B tumor cells was inhibited by 60% compared with cells treated with pTRAIL. Au-PEI/pTRAIL/PEI complexes inhibited cell proliferation by only 30% (Supporting Information, Figure S6). The ability of Au-PEI/pTRAIL/PEI-Dexa to selectively inhibit tumor cell proliferation suggests its in vivo applicability for gene therapy.

To analyze its in vivo activity, one mouse was administered 50 μL of Au-PEI/pTRAIL/PEI-Dexa polyplexes every 5 d. During the entire course of treatment, these polyplexes showed no indications of cytotoxicity, as seen by measuring mouse weight (Figure 9A). Treatment with Au-PEI/pTRAIL/PEI-Dexa complexes significantly inhibited tumor growth, with tumor weight reduced to about 0.2 g after 30 d (Figure 9B), and average tumor reduced to about 300 mm^3, significantly smaller than the average tumor sizes of mice treated with control polyplex (Au-PEI/pTRAIL/PEI) (400 mm^3) or pTRAIL (1000 mm^3) (Figure 9C,D).

To determine whether Dexa residues are the primary factors that enhance transfection efficiency in vivo, we sacrificed tumor-bearing mice and assayed the tumors immunohistochemically with antibody against Flag-TRAIL. Staining was strong in tumor cells, with TRAIL focally expressed in their nuclei (Figure 9E). Compared with the tumor cells of mice treated with pTRAIL only, those from mice treated with complex displayed a strong brown signal in the region of the nuclei. Notably, Au-PEI/pTRAIL/PEI-Dexa treated tumors showed significantly higher Flag-TRAIL expression than Au-PEI/pTRAIL/PEI treated tumors, suggesting that the targeting-Dexa residues resulted in significant expression in tumor cells.

We also examined pTRAIL expression with Western blot, as shown in Figure 9F. Au-PEI/pTRAIL/PEI-Dexa treated tumor cells expressed significantly more TRAIL, and β-actin served as loading control. Furthermore, we sacrificed experiment mice

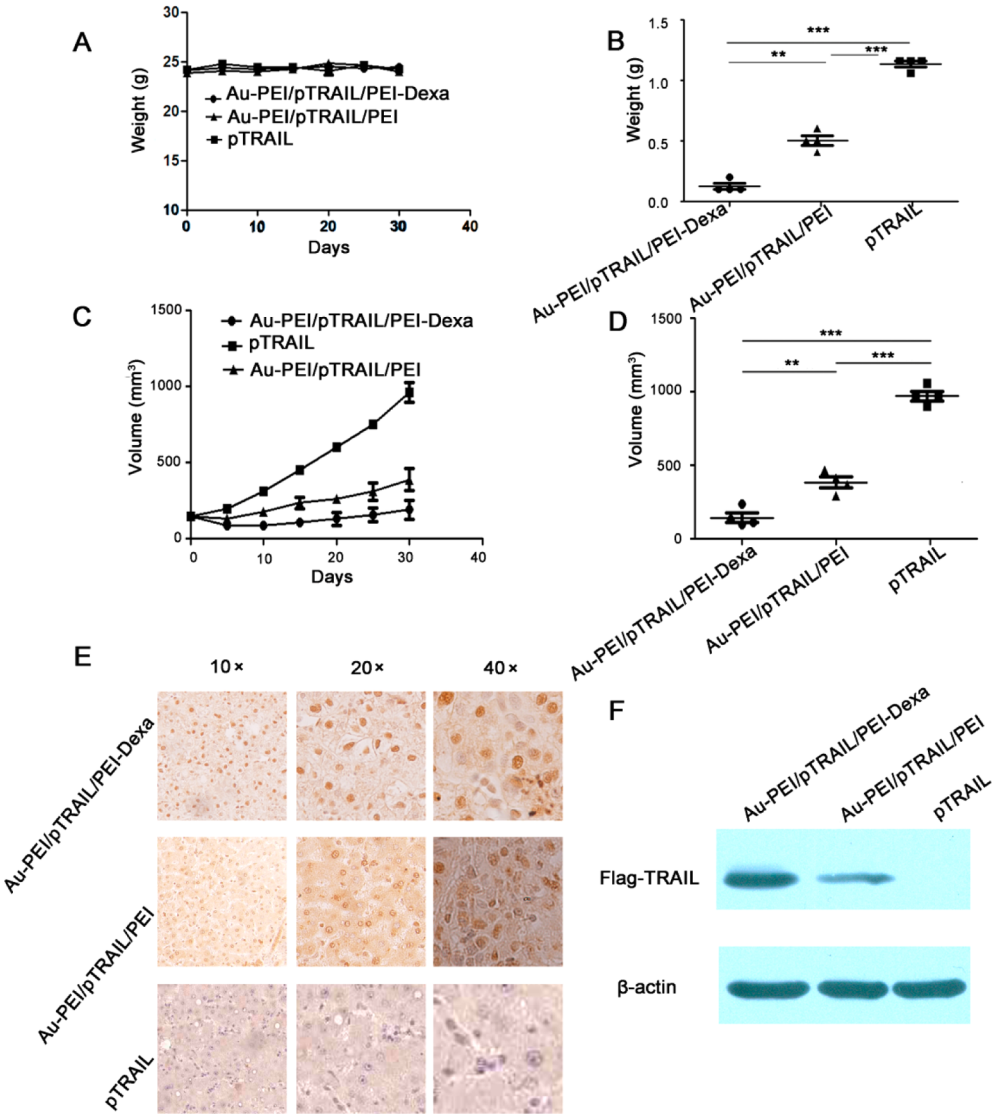

Figure 9. Evaluation of the Au-based nanocomplexes in vivo. (A) Change of mouse weight during systemic administration of the nanocomplexes. (B) When the volume of tumors reached 65 mm^3, Au-PEI/pTRAIL/PEI-Dexa, Au-PEI/pTRAIL/PEI, or pTRAIL only was injected into tumors every 5 d, and tumor volumes were detected every 5 d. The volume curve of tumors was shown. (C, D) 30 d later, the mice were sacrificed, and the tumors were obtained. The weight and volume of tumors were measured by electronic balance and vernier caliper, respectively. (E) Tumors were obtained and prepared for paraffin section, and then immunohistochemical staining of Flag-TRAIL was performed by standard procedure. (F) Tumors were digested and analyzed by Western blotting, Flag was used to indicate the expression of Flag-TRAIL, and β-actin served as loading control. Data are presented as mean values ± SD (n = 3, **: $p < 0.01$; ***: $p < 0.001$).

and control mice, obtained many organs, and examined TRAIL expression by real-time PCR. We found in normal organs the expression of TRAIL was little, if any, while in tumor the expression of TRAIL was extremely high (Supporting Information, Figure S7). This result may be a reason for no side effects and high tumor eliminating capacity of Au-PEI/pTRAIL/PEI-Dexa.

CONCLUSIONS

In summary, we have demonstrated the successful synthesis of nucleus-targeting sandwich-type Au-PEI/DNA/PEI-Dexa ternary complexes via a simple layer-by-layer assembly method using low molecular weight PEI (1.2 kDa) as a mild reducing agent to modify gold nanoparticles. The ternary complex (w/w/w, 0.6/1/2) displayed a high ability to bind DNA, a low charge density, suitable size, and was able to protect DNA against degradation by DNase I. The in vitro transfection of Au-PEI/DNA/PEI-Dexa into Hep3B and 293T cells resulted in low cytotoxicity as well as significantly higher transfection efficiency than the commercial reagent PEI-25kD. The transfection efficiency of the complex likely results from the nucleus-targeting effect of Dexa, which was confirmed by cellular uptake and intracellular trafficking studies. The success of these sandwich-type ternary complexes as transfection vectors was shown to involve the endosomal escape of DNA. Furthermore, immunohistochemistry and Western blotting studies showed that in vivo targeting of the therapeutic agent Flag-tagged TRAIL to Hep3B tumor cells by Au-PEI/pTRAIL/PEI-Dexa significantly inhibited tumor growth in vivo with minimal side effects. These findings suggest that the nucleus-targeting Au-PEI/DNA/PEI-Dexa ternary complexes have promising potential in gene delivery.

■ ASSOCIATED CONTENT

Supporting Information

^{1}H NMR spectrum of PEI-Dexa, UV−vis spectra of the Au-based DNA complexes, cell viability of 293T determined by MTT assay, gene delivery efficiency of complexes on 293T cells, the effect of DNA content on the transfection efficiency of Au-PEI/DNA/PEI-Dexa on Hep3B cells, toxicity of Au-PEI/pTRAIL/PEI-Dexa, Au-PEI/pTRAIL/PEI and pTRAIL on Hep3B tumor cells, the expression of TRAIL in many organs detected by real-time PCR. This material is available free of charge via the Internet at http://pubs.acs.org.

■ AUTHOR INFORMATION

Corresponding Authors

*E-mail: lfzhang@lzu.edu.cn. (L.Z.)

*E-mail: liyf@lzu.edu.cn. Phone: +86-0931-8912528. (Y.L.)

Notes

The authors declare no competing financial interest.

■ ACKNOWLEDGMENTS

This work was supported by grants from the National Natural Science Foundation of China (21104029, 21074049), the Gansu Province Science Foundation for Youth (1107RJYA038), and Fundamental Research Funds for the Central Universities (lzujbky-2013-68). We thank Prof. Y. Shen from Zhejiang University very much for helpful discussion of the rational design for gene delivery vectors.

■ REFERENCES

(1) Corsi, K.; Chellat, F.; Yahia, L.; Fernandes, J. C. Mesenchymal Stem Cells, MG63 and HEK293 Transfection Using Chitosan-DNA Nanoparticles. *Biomaterials* **2003**, *24*, 1255−1264.

(2) Cebrian, V.; Martin-Saavedra, F.; Yague, C.; Arruebo, M.; Santamaria, J.; Vilaboa, N. Size-Dependent Transfection Efficiency of PEI-coated Gold Nanoparticles. *Acta Biomater.* **2011**, *7*, 3645−3655.

(3) Pack, D. W.; Hoffman, A. S.; Pun, S.; Stayton, P. S. Design and Development of Polymers for Gene Delivery. *Nat. Rev. Drug Discovery* **2005**, *4*, 581−593.

(4) Read, M. L.; Logan, A.; Seymour, L. W. In *Non-Viral Vectors for Gene Therapy,* 2nd ed; Huang, L., Hung, M., Wagner, E., Eds.; Elsevier: San Diego, CA, 2005; Part 1, Vol *53*, pp 19−46.

(5) Ogris, M.; Walker, G.; Blessing, T.; Kircheis, R.; Wolschek, M.; Wagner, E. Tumor-Targeted Gene Therapy: Strategies for the Preparation of Ligand−Polyethylene Glycol−Polyethylenimine/DNA Complexes. *J. Controlled Release* **2003**, *91*, 173−181.

(6) Chabaud, P.; Camplo, M.; Payet, D.; Serin, G.; Moreau, L.; Barthelemy, P.; Grinstaff, M. W. Cationic Nucleoside Lipids for Gene Delivery. *Bioconjugate Chem.* **2006**, *17*, 466−472.

(7) Malhotra, M.; Tomaro-Duchesneau, C.; Prakash, S. Synthesis of TAT Peptide-Tagged PEGylated Chitosan Nanoparticles for SiRNA Delivery Targeting Neurodegenerative Diseases. *Biomaterials* **2013**, *34*, 1270−1280.

(8) Wood, K. C.; Little, S. R.; Langer, R.; Hammond, P. T. A Family of Hierarchically Self-assembling Linear-Dendritic Hybrid Polymers for Highly Efficient Targeted Gene Delivery. *Angew. Chem., Int. Ed.* **2005**, *44*, 6704−6708.

(9) Li, S.; Huang, L. Nonviral Gene Therapy: Promises and Challenges. *Gene Ther.* **2000**, *7*, 31−34.

(10) Merdan, T.; Kopecek, J.; Kissel, T. Prospects for Cationic Polymers in Gene and Oligonucleotide Therapy Against Cancer. *Adv. Drug Delivery Rev.* **2002**, *54*, 715−758.

(11) Peng, Z.; Wang, C.; Fang, E.; Lu, X.; Wang, G.; Tong, Q. Co-Delivery of Doxorubicin and SATB1 shRNA by Thermosensitive Magnetic Cationic Liposomes for Gastric Cancer Therapy. *PloS One* **2014**, *9*, e92924.

(12) Boyer, C.; Priyanto, P.; Davis, T. P.; Pissuwan, D.; Bulmus, V.; Kavallaris, M.; Teoh, W. Y.; Amal, R.; Carroll, M.; Woodward, R.; St Pierre, T. Anti-Fouling Magnetic Nanoparticles for SiRNA Delivery. *J. Mater. Chem.* **2010**, *20*, 255−265.

(13) Rosi, N. L.; Giljohann, D. A.; Thaxton, C. S.; Lytton-Jean, A. K. R.; Han, M. S.; Mirkin, C. A. Oligonucleotide-Modified Gold Nanoparticles for Intracellular Gene Regulation. *Science* **2006**, *312*, 1027−1030.

(14) Xu, C.; Yang, D. R.; Mei, L.; Lu, B. G.; Chen, L. B.; Li, Q. H.; Zhu, H. Z.; Wang, T. H. Encapsulating Gold Nanoparticles or Nanorods in Graphene Oxide Shells as a Novel Gene Vector. *ACS Appl. Mater. Interfaces* **2013**, *5*, 2715−2724.

(15) Gemeinhart, R. A.; Luo, D.; Saltzman, W. M. Cellular Fate of A Modular DNA Delivery System Mediated by Silica Nanoparticles. *Biotechnol. Prog.* **2005**, *21*, 532−537.

(16) Boisselier, E.; Astruc, D. Gold Nanoparticles in Nanomedicine: Preparations, Imaging, Diagnostics, Therapies and Toxicity. *Chem. Soc. Rev.* **2009**, *38*, 1759−1782.

(17) Ghosh, P.; Han, G.; De, M.; Kim, C. K.; Rotello, V. M. Gold Nanoparticles in Delivery Applications. *Adv. Drug Delivery Rev.* **2008**, *60*, 1307−1315.

(18) Giljohann, D. A.; Seferos, D. S.; Daniel, W. L.; Massich, M. D.; Patel, P. C.; Mirkin, C. A. Gold Nanoparticles for Biology and Medicine. *Angew. Chem., Int. Ed.* **2010**, *49*, 3280−3294.

(19) Ghosh, P. S.; Kim, C. K.; Han, G.; Forbes, N. S.; Rotello, V. M. Efficient Gene Delivery Vectors by Tuning the Surface Charge Density of Amino Acid-Functionalized Gold Nanoparticles. *ACS Nano* **2008**, *2*, 2213−2218.

(20) Thomas, M.; Klibanov, A. M. Conjugation to Gold Nanoparticles Enhances Polyethylenimine's Transfer of Plasmid DNA into Mammalian Cells. *Proc. Natl. Acad. Sci. U.S.A.* **2003**, *100*, 9138−9143.

(21) Sandhu, K. K.; McIntosh, C. M.; Simard, J. M.; Smith, S. W.; Rotello, V. M. Gold Nanoparticle-Mediated Transfection of Mammalian Cells. *Bioconjugate Chem.* **2002**, *13*, 3−6.

(22) Niidome, T.; Nakashima, K.; Takahashi, H.; Niidome, Y. Preparation of Primary Amine-Modified Gold Nanoparticles and Their Transfection Ability into Cultivated Cells. *Chem. Commun.* **2004**, 1978−1979.

(23) Li, P. C.; Li, D.; Zhang, L. X.; Li, G. P.; Wang, E. K. Cationic Lipid Bilayer Coated Gold Nanoparticles-Mediated Transfection of Mammalian Cells. *Biomaterials* **2008**, *29*, 3617−3624.

(24) Boussif, O.; Lezoualch, F.; Zanta, M. A.; Mergny, M. D.; Scherman, D.; Demeneix, B.; Behr, J. P. A Versatile Vector for Gene and Oligonucleotide Transfer into Cells in Culture and in Vivo Polyethylenimine. *Proc. Natl. Acad. Sci. U.S.A.* **1995**, *92*, 7297−7301.

(25) Godbey, W. T.; Wu, K. K.; Mikos, A. G. Tracking the Intracellular Path of Poly(ethylenimine)/DNA Complexes for Gene Delivery. *Proc. Natl. Acad. Sci. U.S.A.* **1999**, *96*, 5177−5181.

(26) Hu, C.; Peng, Q.; Chen, F. J.; Zhong, Z. L.; Zhuo, R. X. Low Molecular Weight Polyethylenimine Conjugated Gold Nanoparticles as Efficient Gene Vectors. *Bioconjugate Chem.* **2010**, *21*, 836−843.

(27) Chen, S.; Li, F.; Zhuo, R. X.; Cheng, S. X. Efficient Non-Viral Gene Delivery Mediated by Nanostructured Calcium Carbonate in Solution-Based Transfection and Solid-Phase Transfection. *Mol. BioSyst.* **2011**, *7*, 2841−2847.

(28) Nishikawa, M.; Huang, L. Nonviral Vectors in the New Millennium: Delivery Barriers in Gene Transfer. *Hum. Gene Ther.* **2001**, *12*, 861−870.

(29) Adcock, I. M.; Caramori, G. Cross-Talk between Pro-Inflammatory Transcription Factors and Glucocorticoids. *Immunol. Cell Biol.* **2001**, *79*, 376−384.

(30) Shahin, V.; Albermann, L.; Schillers, H.; Kastrup, L.; Schafer, C.; Ludwig, Y.; Stock, C.; Oberleithner, H. Steroids Dilate Nuclear Pores Imaged with Atomic Force Microscopy. *J. Cell. Physiol.* **2005**, *202*, 591−601.

(31) Sun, X.; Dong, S.; Wang, E. One-step Preparation of Highly Concentrated Well-Stable Gold Colloids by Direct Mix of Polyelectrolyte and HAuCl4 Aqueous Solutions at Room Temperature. *J. Colloid Interface Sci.* **2005**, *288*, 301−303.

(32) Godbey, W. T.; Wu, K. K.; Mikos, A. G. Poly(ethylenimine) and Its Role in Gene Delivery. *J. Controlled Release* **1999**, *60*, 149−160.
(33) Elbashir, S. M.; Harborth, J.; Lendeckel, W.; Yalcin, A.; Weber, K.; Tuschl, T. Duplexes of 21-Nucleotide RNAs Mediate RNA Interference in Cultured Mammalian Cells. *Nature* **2001**, *411*, 494−498.
(34) Qin, X. F.; An, D. S.; Chen, I. S. Y.; Baltimore, D. Inhibiting HIV-1 Infection in Human T Cells by Lentiviral-Mediated Delivery of Small Interfering RNA Against CCR5. *Proc. Natl. Acad. Sci. U.S.A.* **2003**, *100*, 183−188.
(35) Schmalenberg, K. E.; Frauchiger, L.; Nikkhouy-Albers, L.; Uhrich, K. E. Cytotoxicity of A Unimolecular Polymeric Micelle and Its Degradation Products. *Biomacromolecules* **2001**, *2*, 851−855.
(36) Sonawane, N. D.; Szoka, F. C.; Verkman, A. S. Chloride Accumulation and Swelling in Endosomes Enhances DNA Transfer by Polyamine-DNA Polyplexes. *J. Biol. Chem.* **2003**, *278*, 44826−44831.
(37) Ashkenazi, A.; Dixit, V. M. Death Receptors: Signaling and Modulation. *Science* **1998**, *281*, 1305−1308.
(38) Ashkenazi, A.; Pai, R. C.; Fong, S.; Leung, S.; Lawrence, D. A.; Masters, S. A.; Blackie, C.; Chang, L.; McMurtrey, A. E.; Hebert, A.; DeForge, L.; Koumenis, I. L.; Lewis, D.; Harris, L.; Bussiere, J.; Koeppen, H.; Shahrokh, Z.; Schwall, R. H. Safety and Antitumor Activity of Recombinant Soluble Apo2 Ligand. *J. Clin. Invest.* **1999**, *104*, 155−162.
(39) Zhou, J. B.; Liu, J.; Cheng, C. J.; Patel, T. R.; Weller, C. E.; Piepmeier, J. M.; Jiang, Z. Z.; Saltzman, W. M. Biodegradable Poly(amine-co-ester) Terpolymers for Targeted Gene Delivery. *Nat. Mater.* **2012**, *11*, 82−90.
(40) Kagawa, S.; He, C.; Gu, J.; Koch, P.; Rha, S. J.; Roth, J. A.; Curley, S. A.; Stephens, L. C.; Fang, B. L. Antitumor Activity and Bystander Effects of the Tumor Necrosis Factor-Related Apoptosis-Inducing Ligand (TRAIL) Gene. *Cancer Res.* **2001**, *61*, 3330−3338.